ARTICLE
Journal of Cellular Biochemistry 114:212–219 (2013)

Journal of Cellular Biochemistry

Mitochondrial Accumulation Under Oxidative Stress is Due to Defects in Autophagy

Cheng Luo,[1] Yan Li,[2] Hui Wang,[1] Zhihui Feng,[1] Yuan Li,[1] Jiangang Long,[1*] and Jiankang Liu[1*]

[1]*Institute of Mitochondrial Biology and Medicine, The Key Laboratory of Biomedical Information Engineering of Ministry of Education, Xi'an Jiaotong University School of Life Science and Technology, Xi'an 710049, China*

[2]*Center for Bioinformatics, The Key Laboratory of Biomedical Information Engineering of Ministry of Education, Xi'an Jiaotong University School of Life Science and Technology, Xi'an 710049, China*

ABSTRACT

Mitochondrial dynamics maintains normal mitochondrial function by degrading damaged mitochondria and generating newborn mitochondria. The accumulation of damaged mitochondria influences the intracellular environment by promoting mitochondrial dysfunction, and thus initiating a vicious cycle. Oxidative stress induces mitochondrial malfunction, which is involved in many cardiovascular diseases. However, the mechanism of mitochondrial accumulation in cardiac myoblasts remains unclear. We observed mitochondrial dysfunction and an increase in mitochondrial mass under the oxidative conditions produced by *tert*-butyl hydroperoxide (tBHP) in cardiac myoblast H9c2 cells. However, in contrast to the increase in mitochondrial mass, mitochondrial DNA (mtDNA) decreased, suggesting that enhanced mitochondrial biogenesis may be not the primary cause of the mitochondrial accumulation. Therefore, we investigated changes in a number of proteins involved in autophagy. Beclin1, Atg12–Atg5 conjugate, Atg7 contents decreased but LC3-II accumulated in tBHP-treated H9c2 cells. Moreover, the capacity for acid hydrolysis decreased in H9c2 cells. We also demonstrated a decrease in DJ-1 protein under the oxidative conditions that deregulate mitochondrial dynamics. These results reveal that autophagy became defective under oxidative stress. We therefore suggest that defects in autophagy mediate mitochondrial accumulation under these conditions. J. Cell. Biochem. 114: 212–219, 2013.

KEY WORDS: AUTOPHAGY; *TERT*-BUTYL HYDROPEROXIDE (tBHP); MITOCHONDRIAL MASS; MITOCHONDRIAL DNA (mtDNA); MITOCHONDRIAL BIOGENESIS; OXIDATIVE STRESS

Mitochondria couple oxidative phosphorylation with respiration to satisfy most energy requirements for cells to metabolize and proliferate. In addition, mitochondria play vital roles in the production of endogenous reactive oxygen species (ROS) and in apoptosis. Thus, mitochondria play critical roles in both cell life and death. Mitochondrial functions vary with changes in their shape, size, and abundance in different environments. Mitochondrial dynamics, including mitochondrial biogenesis, fusion, fission, transport, and mitophagy, is involved in many diseases [Zorzano et al., 2009a], such as obesity [Zorzano et al., 2009b], diabetes [Yoon et al., 2011], neurodegenerative diseases [Chen and Chan, 2009], and cardiovascular disease [Hausenloy and Ong, 2010; Rothermel et al., 2010; Lavandero et al., 2011]. Involvement of mitochondrial dynamics is especially notable when the pathological changes occurring in these diseases are associated with oxidative stress.

Mitochondria are not only the main intracellular sources for ROS, but also the immediate targets. Oxidative stress induces mitochondrial fragmentation and dysfunction. Many researchers have found that mitochondrial mass increases under conditions of oxidative stress [Lee et al., 2000, 2002, 2005; Apostolova et al., 2010]. Mitochondrial biogenesis and involvement of protein kinase Cδ are considered to be the main causes of increases in mitochondrial mass and DNA (mtDNA) [Lee and Wei, 2005; Lee et al., 2006].

Autophagy is a process by which cells regulate the turnover of long-lived proteins and eliminate dysfunctional organelles. The autophagosome, a structure bounded by a double-membrane, matures by fusion with lysosomes. Following fusion, autolysosomes and lysosomes can then release the acidic hydrolases that digest waste materials [Uchiyama et al., 2008]. The selective autophagy of mitochondria is called mitophagy [Lemasters, 2005] and is a process

Grant sponsor: National Natural Science Foundation of China; Grant numbers: 30930105, 31070740; Grant sponsor: New Century Excellent Talents in University.

*Correspondence to: Jiangang Long or Jiankang Liu, Institute of Mitochondrial Biology and Medicine, Xi'an Jiaotong University School of Life Science and Technology, Xi'an 710049, China.
E-mail: jglong@mail.xjtu.edu.cn; j.liu@mail.xjtu.edu.cn

Manuscript Received: 24 March 2012; Manuscript Accepted: 7 August 2012
Accepted manuscript online in Wiley Online Library (wileyonlinelibrary.com): 17 August 2012
DOI 10.1002/jcb.24356 • © 2012 Wiley Periodicals, Inc.

common to yeast and mammals [Tolkovsky, 2009; Goldman et al., 2010]. Mitophagy can eliminate damaged mitochondria and thus help prevent cell death [Codogno and Meijer, 2005]. Dysfunction of autophagy results in the accumulation of waste materials and mitochondria, and in consequence induces aging [Stroikin et al., 2004], neurodegenerative diseases [Cuervo and Wong, 2010], muscle disorders [Long et al., 2010], and heart diseases [Otsu et al., 2007].

Aberrant mitochondrial biogenesis may cause an increase in mitochondrial mass [Lee and Wei, 2005]. Furthermore, a recent review suggests that effective quality control of mitochondria should involve maintenance of a balance between biogenesis of healthy mitochondria and degradation of dysfunctional mitochondria [Michel et al., 2011]. Oxidative stress plays a vital role in the pathogenesis of heart failure, accompanied by mitochondrial damage [Nojiri et al., 2006; Dai et al., 2011]. The rat cardiac myoblast cell line H9c2 is used frequently as an in vitro cardiovascular diseases model, mainly because its response to stimulative stress is similar to that of primary neonatal cardiomyocyte cells [Watkins et al., 2011]. We hypothesize that defects in autophagy are the primary factors underlying damage to cardiac myoblasts resulting from acute oxidative stress. To test this, we exposed cardiac myoblast H9c2 cells to oxidative stress by treatment with *tert*-butyl hydroperoxide (tBHP), and then measured mitochondrial mass and mtDNA content, and assessed changes in autophagic function.

MATERIALS AND METHODS

MATERIALS

High glucose Dulbecco's modified Eagle's medium (DMEM), penicillin, streptomycin, MitoTracker® Green FM, LysoTracker Red DND-99, trypsin, Acridine Orange (AO) and 5,5′,6,6′-tetrachloro-1,1′,3,3′-tetraethylbenzimidazolylcarbocyanine iodide (JC-1; CBIC2(3)) were purchased from Invitrogen (Carlsbad, CA). tBHP was obtained from Sigma (St Louis, MO). HRP conjugated anti-mouse/rabbit/goat IgG antibodies and fetal bovine serum (FBS) were purchased from Jackson ImmunoResearch Laboratories (West Grove, PA) and PAA Laboratories GmbH (Linz, Austria), respectively.

CELL CULTURE AND TREATMENT

Rat cardiac myoblast H9c2 cells were cultured in high glucose DMEM medium containing 10% FBS, 100 units/ml penicillin and 100 μg/ml streptomycin. Cell cultures were maintained in a 37°C, humidified 5% CO_2 incubator (Thermo Fisher Scientific, Inc., Waltham, MA). H9c2 cells were treated either with different concentrations (0, 100, 200, 300, or 400 μmol/L) of tBHP for 4 h, or with 300 μmol/L tBHP for different time (0, 0.5, 1, 2, 3, or 4 h).

ASSAY FOR MITOCHONDRIAL MASS

Mitochondrial mass were measured with a probe targeting to mitochondria [Agnello et al., 2008]. Briefly, for flow cytometry analysis, cells were detached by trypsin and incubated with 100 nmol/L mitotracker green FM at 37°C for 30 min, and then centrifuged at approximately 300*g* for 5 min at 4°C. The fluorescence labeled cells were suspended in PBS and analyzed by a BD FACSCalibur Flow Cytometry System (excitation: 485 nm; emission: 530 nm) (BD Biosciences, San Diego, CA). For fluorescent images of mitochondria, cells were incubated with 100 nmol/L mitotracker green for 30 min at 37°C, and then washed with PBS three times. The fluorescent images of mitochondria were recorded with a fluorescence microscope (Olympus IX71).

ASSAY FOR MITOCHONDRIAL MEMBRANE POTENTIAL

Cells were detached by trypsin and incubated with 5 μmol/L JC-1 at 37°C for 30 min, and then centrifuged at approximately 300*g* for 5 min at 4°C. The fluorescence labeled cells were suspended in PBS and analyzed by a BD FACSCalibur Flow Cytometry System (excitation: 485 nm; emission: 530 nm, 590 nm) (BD Biosciences). The ratio of fluorescence at 590 nm versus 530 nm emission was used for quantitating the mitochondrial membrane potential, just as described previously [Salvioli et al., 1997] and instructions from invitrogen.

ASSAY FOR OXYGEN CONSUMPTION RATE

Intracellular oxygen consumption rate was assessed using a BD Oxygen Biosensor System (BD Biosciences) [Guarino et al., 2004]. According to the manufacturer's instructions, cells were detached and suspended in fresh media in BD Oxygen Biosensor System plate (BD Biosciences). The plate was sealed with parafilm and recorded by a plate reader (Thermo Fluoroskan Ascent FL) at 37°C for 30 min (excitation: 485 nm; emission: 630 nm). The fluorescence data, due to the reaction of ruthenium-based fluorophore (tris 4,7-diphenyl-1,10-phenanthroline ruthenium (II) chloride ($Ru(DPP)_3Cl_2$)) and dissolved oxygen, were normalized by cell numbers which were determined by hemacytometer counts.

ASSAY FOR INTRACELLULAR ADENOSINE 5′-TRIPHOSPHATE (ATP) LEVELS

ATP contents were assayed based on a bioluminometric assay method [Khan, 2003]. Briefly, cells were lysed by 0.5% Triton X-100 in 100 mmol/L glycine buffer (pH 7.4), and then centrifuged at approximately 15,000*g* for 10 min at 4°C. According to the manufacturer's instructions, the supernatants were removed and transferred to ATP assay mix working solution (Sigma), and the amount of light emitted was measured with a luminometer (Thermo Scientific Luminoskan Ascent) immediately. The luminescence data were normalized by sample protein amounts.

ASSAY FOR MITOCHONDRIAL DNA CONTENT

Mitochondrial DNA (mtDNA) was assessed by real-time quantitative PCR, using 18S rRNA as an endogenous reference gene and mitochondrial D-loop as target gene, just as described previously [Shen et al., 2008]. Each volume of quantitative PCR reaction mixture (10 μl) contained 5 μl SYBR Premix Ex Taq™ from TaKaRa Biotechnology (Dalian) Co., Ltd, 0.5 μl of each primer (10 pmol/L) and 2.5 ng template (DNA) or no template (NTC), and RNase-free water. The conditions for PCR were: initial denaturation at 95°C for 5 min, followed by 40 cycles of 95°C for 30 s, 55°C for 30 s and 72°C for 20 s. Mitochondrial D-loop forward, 5′-AAGTGGCTGTGCAGACATTC-3′, reverse 5′-TCTGTCTTTGATTCCTGCCT-3′; and 18S rRNA

forward: 5′-TCTCCTACTTGGATAACTGTGG-3′, reverse: 5′-GGCGACTACCATCGAAAGTTG-3′, were used as primer pairs. mtDNA content was determined as the ratio of mitochondrial D-loop to 18S rRNA.

VISUALIZATION OF AUTOPHAGIC VACUOLES (AUTOPHAGOSOMES AND AUTOLYSOSOMES)

Monodansylcadaverine (MDC) is incorporated selectively into autophagosomes and autolysosomes, and where its fluorescence detects autophagic vacuoles [Biederbick et al., 1995]. Aggregates of AO fluoresce bright red in the acidic environment of autophagic vacuoles, but fluoresce bright green in the cytoplasm and nucleus [Stankiewicz et al., 1996]. Lysotracker red labels acidic organelles (mainly lysosomes) [Chazotte, 2011]. Briefly, cells were incubated with 50 μmol/L MDC, 5 μg/ml AO, or 50 nmol/L lysotracker red for 15 min at 37°C, and then washed with PBS three times. The fluorescent images of autophagic vacuoles were recorded with a fluorescence microscope (Olympus IX71).

WESTERN BLOT ANALYSIS

H9c2 cells were lysed with buffer (Beyotime Biotechonology) at 4°C for 30 min and centrifuged at 17,000*g* for 15 min. The BCA™ Protein Assay kit was used to determine protein concentrations. Samples of about 20 μg protein were separated by SDS polyacrylamide gel electrophoresis. Proteins were transferred to nitrocellulose membranes (Millipore) and blocked with 5% nonfat milk/TBST. The membranes were incubated with primary antibodies against Beclin1, Atg12, Atg7, LC3 (cell signaling), β-actin (Sigma), OxPhos Complex I subunit NDUFS3, OxPhos Complex II 30 kDa subunit, OxPhos Complex II 70 kDa subunit, OxPhos Complex III subunit core 1, OxPhos Complex IV subunit I, OxPhos Complex V (F1F0-ATP synthase) subunit α (Invitrogen) and followed by incubation with secondary antibody for 1 h at room temperature. Western blots were developed using chemiluminescent HRP substrate.

STATISTICAL ANALYSIS

Data represent means ± SEM from at least three independent experiments. The data were analyzed using IBM SPSS Statistics. For three or more than three experimental groups, one-way analysis of variance (ANOVA) followed by Fisher's LSD test was used to evaluate statistical significance of differences; moreover, for two experimental groups, Student's test was used to assess statistical significance of differences. Significant changes are denoted as follows: $^{*}P < 0.05$; $^{**}P < 0.01$.

RESULTS

MITOCHONDRIAL DYSFUNCTION AND ACCUMULATION OF MITOCHONDRIA

We verified that cardiac myoblast mitochondria become dysfunctional when subjected to oxidative stress, as has been reported previously many times. There were significant decreases in mitochondrial membrane potential, oxygen consumption, and intracellular ATP content. However, mitochondrial mass increased when cardiac myoblast H9c2 cells were treated with 300 μmol/L tBHP for 4 h (Fig. 1a,b). To confirm the abnormal increase in mitochondrial mass, levels of respiratory chain complex proteins were assessed by Western blot analysis. After H9c2 cells were treated

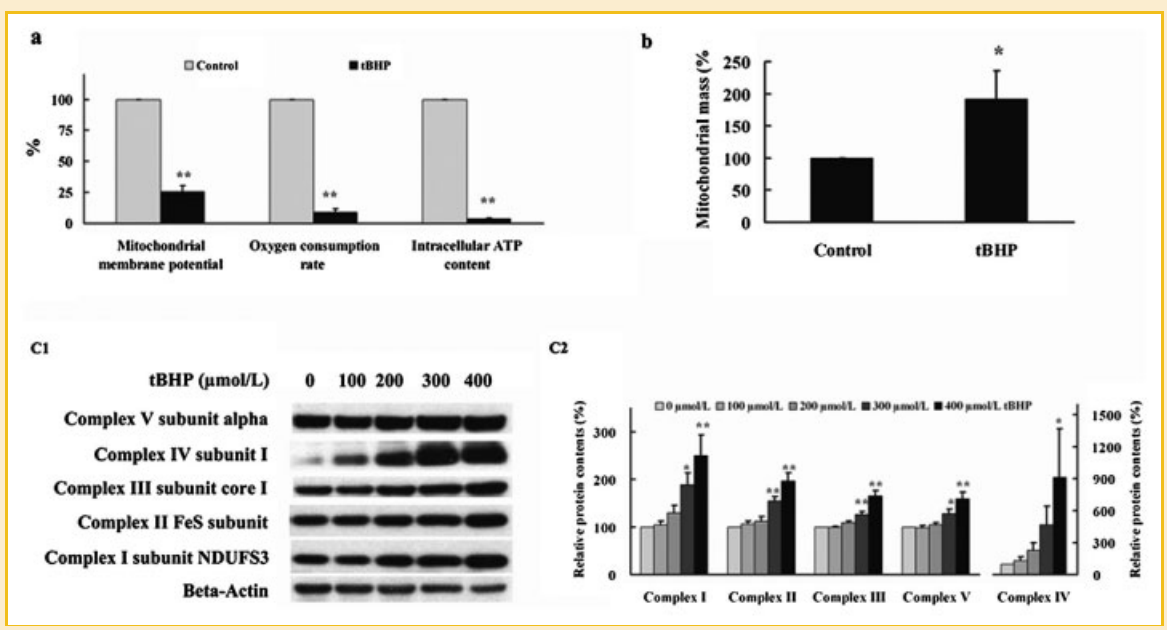

Fig. 1. Mitochondrial dysfunction and increased mitochondrial mass in H9c2 cells treated with *tert*-butyl hydroperoxide (tBHP). H9c2 cells were treated with 300 μmol/L tBHP for 4 h, and then (a) mitochondrial function: mitochondrial membrane potential (n = 7), oxygen consumption rate (n = 5) and intracellular ATP level (n = 7), and (b) mitochondrial mass (n = 3) were measured. $^{*}P < 0.05$ $^{**}P < 0.01$ versus Control. c: Western blot analysis of mitochondrial respiratory chain complexes I, II, III, IV, and V. c1: Representative blots from eight different experiments. c2: Semi-quantified statistics. The semi-quantified statistics for Western blot was analyzed by Quantity One software and normalized with β-actin. $^{*}P < 0.05$, $^{**}P < 0.01$ versus untreatment group.

with tBHP for 4 h, concentration-dependent increases in all respiratory chain complex proteins were observed (Fig. 1c).

MITOCHONDRIAL DNA MAINTENANCE

We evaluated changes in mtDNA contents in response to tBHP treatment in H9c2 cells. Quantitative real-time PCR was used to determine changes in the relative copy number of mtDNA. After cells were treated with a low, non-fatal concentration (100 μmol/L) of tBHP for 4 h, the copy number of mtDNA increased. From that level, however, it decreased in a concentration-dependent manner at higher concentrations ranging from 200 to 400 μmol/L (Fig. 2a). After cells were treated with 300 μmol/L tBHP for various time periods, mtDNA copy number followed a similar but time dependent pattern (Fig. 2b).

AUTOPHAGIC DYSFUNCTION

Initiation, nucleation, and elongation are the early events that promote formation of autophagosomes. We assayed some proteins that play important roles in the formation of autophagosomes in order to assess autophagy status. DJ-1, a protein associated with Parkinson's disease, regulates autophagic progression in many cells. Microtubule-associated protein light chain 3 II (LC3-II) is widely used for monitoring autophagic flux. As shown in Figure 3a, treatment of H9c2 cells with tBHP induced remarkable concentration-dependent decreases in levels of Beclin1, the Atg12–Atg5 conjugation complex, Atg7 and DJ-1. However, exposure of H9c2 cells to tBHP for 4 h resulted in a concentration-dependent decrease of LC3-I accompanied by an accumulation of LC3-II (Fig. 3b).

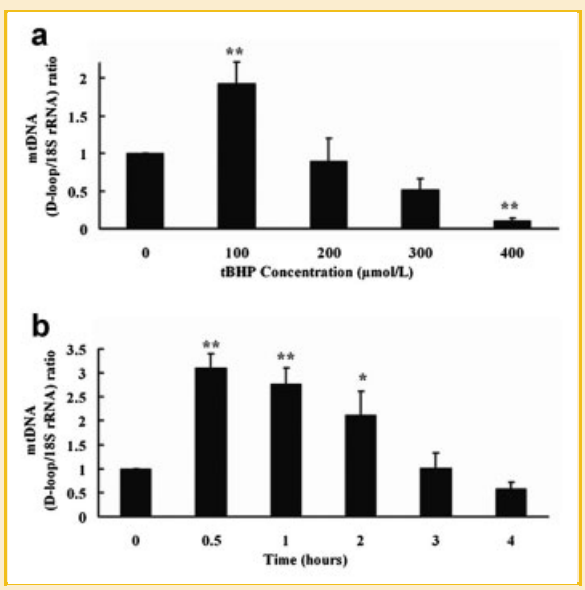

Fig. 2. Mitochondrial DNA (mtDNA) changes in H9c2 cells treated with tBHP. H9c2 cells were treated with (a) 0, 100, 200, 300, or 400 μmol/L tBHP for 4 h ($n = 5$), and (b) 300 μmol/L tBHP for 0, 0.5, 1, 2, 3, or 4 h ($n = 4$); then relative mtDNA contents were determined by Real-time quantitative PCR. $^{*}P < 0.05$ $^{**}P < 0.01$ versus untreated control.

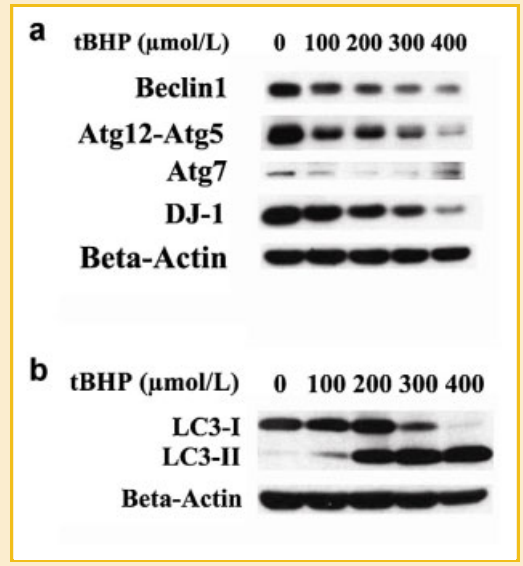

Fig. 3. Autophagy-associated proteins in H9c2 cells treated with tBHP. a: Protein markers for nucleation and elongation of autophagosomes. b: Autophagosome marker LC3. H9c2 cells were treated with 0, 100, 200, 300, or 400 μmol/L tBHP for 4 h, and then autophagy was assessed by Western blot analysis ($n = 4$).

DESTRUCTION OF AUTOPHAGIC VACUOLES AND IMPAIRMENT OF LYSOSOMES

Autophagy consists of five events altogether: initiation, nucleation, elongation, maturation, and degradation. Autophagosomes, autolysosomes, and lysosomes are acidic vesicles, which can degrade materials deposited in the vacuoles. Acidic dyes, MDC, AO, and lysotracker red, were used to stain autophagic vacuoles and lysosomes specifically. As shown in Figure 4, there were concentration- and time-dependent decreases in fluorescent intensities in tBHP-treated H9c2 cells, showing impairment in autophagic degradation. Relevant to cessation of lysosome activity, there was a remarkable increase in mitochondrial mass (Fig. 4a3,b3).

DISCUSSION

Oxidative stress stimulates changes in mitochondrial mass and mtDNA [Lee et al., 2000, 2002, 2005; Apostolova et al., 2010]. Wei and coworkers have summarized the factors enhancing mitochondrial biogenesis [Lee and Wei, 2005]. However, oxidative stress nearly always induces mitochondrial dysfunction and ROS production [Ballinger, 2005; Beal and Lin, 2006; Victor et al., 2009], except for one study in human cells conducted in Yau-Huei Wei's lab [Lee et al., 2000]. Autophagy plays a vital role in the clearance of dysfunctional mitochondria [Tolkovsky, 2009; Goldman et al., 2010]. The aim of the present work was to explore the phenomenon of mitochondrial mass increase induced by oxidative stress from a perspective differing from that reported by the Wei lab in a later study [Lee and Wei, 2005].

Our results imply a mechanism differing from the one reported by the Wei lab. We believe that this difference in mechanism may be

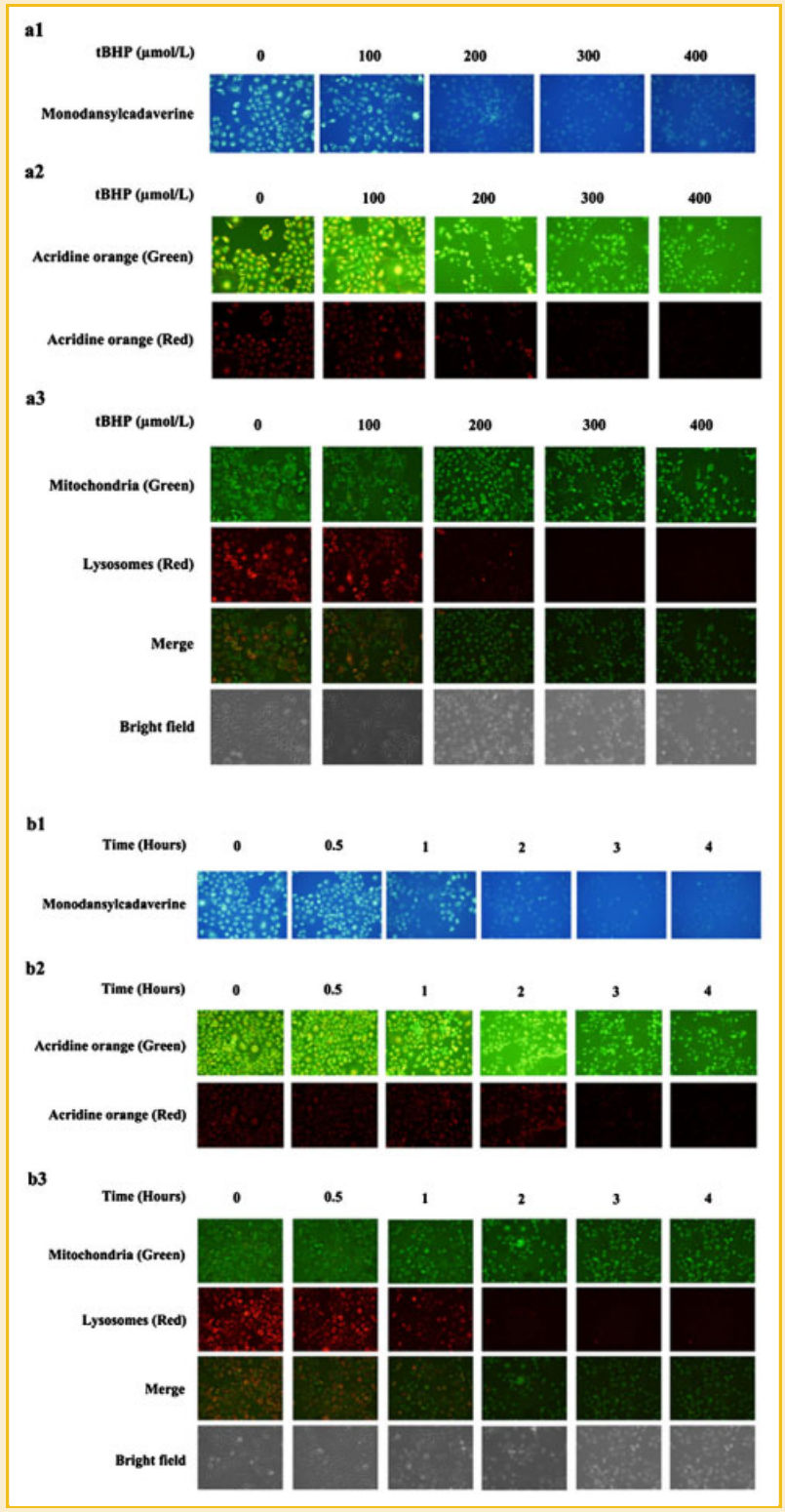

Fig. 4. Autophagosome maturation and presence of lysosomes. a: H9c2 cells were treated with 0, 100, 200, 300, or 400 μmol/L tBHP for 4 h, and then formation of autophagic vacuoles was assessed with monodansylcadaverine (MDC) and acridine orange (AO) staining, and densities and distribution of mitochondria and lysosomes were assessed with Mitotracker Green FM and LysoTracker Red, respectively. b: H9c2 cells were treated with 300 μmol/L tBHP for 0, 0.5, 1, 2, 3, or 4 h, and then formation of autophagic vacuoles was assessed with MDC and AO staining, and densities and distribution of mitochondria and lysosomes were assessed with Mitotracker Green FM and LysoTracker Red, respectively.

due to differences in the models chosen [Lee et al., 2000, 2002, 2005, 2006; Lee and Wei, 2005]. Our research utilizes an acute stress model, that is, treatment with tBHP for a short time (4 h maximum). However, Wei's group treated their cells for longer times, as long as 72 h. Typically, the length of time and intensity of treatment determine the response pattern cells choose for modulating the physiological changes that minimize damage. Acute heart damage always accompanies myocardial ischemia, so the acute damage model is appropriate for revealing the relevant mechanisms.

Atherosclerosis is the underlying cause of ischemic heart disease, which results in some disorders such as angina pectoris, myocardial infarction, and heart failure. Such disorders invariably lead to acute heart damage, particularly myocardial necrosis. Oxidative stress is the main cause of ischemia-reperfusion (hypoxia-reoxygenation) injury in cardiovascular diseases. The H9c2 cell line, a subclone derived from an embryonic rat ventricle [Kimes and Brandt, 1976], has been used to investigate the molecule mechanisms underlying the cellular response to oxidative stress. tBHP consists of a tertiary butyl group and a hydridodioxygen group. As an organic hydroperoxide, tBHP is more stable than hydrogen peroxide (H_2O_2), and it selectively inhibits mitochondrial function [Haidara et al., 2002; Drahota et al., 2005; Krivakova et al., 2007], induces membrane lipid peroxidation [Uchida et al., 1994; Gorbunov et al., 1998], and promotes nucleotide degradation and adenosine formation [Andersson et al., 1996]. When H9c2 cells are treated with tBHP, the morphology of their mitochondria changes from long filaments to small, round fragments [Sardao et al., 2007]. Based on the relatively well-defined mechanisms of tBHP action, we chose tBHP-treated H9c2 cells as a biological model likely to result in mitochondrial dysfunction in response to oxidative stress.

Nuclear DNA and mtDNA together regulate mitochondrial protein synthesis to ensure proper mitochondrial assembly. Therefore, mtDNA copy number can be used to evaluate mitochondrial biogenesis. Mitochondrial function was destroyed in H9c2 cells treated with 300 μmol/L tBHP for 4 h (Fig. 1a). Moreover, content of mitochondrial mass and respiratory chain complex proteins increased significantly (Fig. 1b,c). However, the increase of electron transfer subunits was not in a neatly coordinate ratio, which will destroy the correct assembly to be respirasomes (Fig. 1c).

The copy numbers of mtDNA at first quickly increased under oxidative stimulation, but then decreased in a time- and concentration-dependent manner, to levels even less than in the untreated group (Fig. 2). This finding is similar to a report from Shokolenko et al., which provided evidences in oxidatively damaged mtDNA degradation processes. When ROS generates in an enzymatic mode, or base excision repair of oxidative/alkylating DNA damage is inhibited, mtDNA degradation will be induced or enhanced, respectively [Shokolenko et al., 2009]. Taken together, exogenous oxidative stress may impair the replication or accelerate the degradation of mtDNA, resulting in a decrease of mtDNA copy number.

The mammalian mtDNA encodes 13 peptides for electron transfer complex subunits (complex I (ND1, ND2, ND3, ND4, ND4L, ND5, ND6), complex III (Cyt b), complex IV (COI, COII, COIII), and complex V (Atp6, Atp8)) as well as 22 tRNAs and 2 rRNAs (12S, 16S) [Anderson et al., 1981]. Mitochondrial biogenesis is a complex cellular event requiring the coordinated synthesis of proteins encoded on mtDNA and nuclear DNA. When mtDNA content decreases, the ability of mitochondrial biogenesis should accordingly cut down. Mitochondrial dynamics (fission and fusion) regulate the changes in the mitochondrial morphology (discrete tubules or interconnected networks), but not the contents or ratios of mitochondrial components. Taken together, it implies that there is a positive correlation between mtDNA content and mitochondrial mass (or mitochondrial components contents). However, that the changes in mitochondrial mass and mtDNA copy number are in opposite directions indicates that the decrease in mitochondrial degradation, not the increase in mitochondrial biogenesis, may play a more important role in mitochondrial accumulation in response to oxidative stress. Dysfunctional mitochondria can be digested by autophagy (which then may be termed *mitophagy*) [Tolkovsky, 2009]. We utilized Western blot analysis and fluorescence labeling to evaluate autophagic flux.

The steps in the autophagic process include induction, autophagosome formation, maturation, degradation, and materials reuse [He and Klionsky, 2009]. The proteins involved and their stepwise interactions have been identified. Beclin1, a subunit of the class III PI3-kinase complex, participates in membrane nucleation. Atg7, an E1 enzyme that activates ubiquitination, catalyzes the covalent coupling of Atg12 with Atg5. The Atg12–Atg5 conjugate interacts with Atg16 and forms a complex attached to a phagophore. Atg7 and the Atg12–Atg5 conjugate facilitate LC3-I activation. Activated LC3-I then conjugates with the target lipid phosphatidylethanolamine (PE) on the outer membrane, forming LC-II. Finally, LC3-II is cleaved to LC3-I and released back to the cytosol or degraded upon autophagosome maturation [He and Klionsky, 2009]. Autophagosomes mature upon fusion with lysosomes, and are then referred to as autolysosomes or autophagolysosomes. So fused, they employ acid hydrolases to degrade the wastes (which are enclosed in vacuoles) [Mizushima, 2007]. DJ-1, a protein associated with Parkinson's disease, has been implicated in maintaining mitochondrial function under oxidative stress through regulation of autophagy [Zhang et al., 2005; Hayashi et al., 2009; Giasson et al., 2010; Krebiehl et al., 2010; Thomas et al., 2011]. The occurrence of mitochondrial dysfunction in DJ-1-mutant mice [Giasson et al., 2010], the presence of defects in mitochondrial fusion, and the accumulation of markers of autophagy in DJ-1deficient cells [Thomas et al., 2011] suggest that DJ-1 regulates mitochondrial dynamics and autophagy indirectly [Cookson and Mccoy, 2011]. Krebiehl et al. [2010] found that autophagy is impaired in DJ-1-knockout cells, and that dysfunctional mitochondria accumulate in them.

Figure 3a shows significant concentration-dependent decreases in autophagy marker proteins (Beclin1, Atg12–Atg5 conjugation complex and Atg7) in tBHP-treated H9c2 cells. These results indicate that a reduction in autophagosome formation or capacity for autophagy occurred. In contrast, LC3-II, conventionally used for assessing autophagic flux, increased in a concentration-dependent manner (Fig. 3b). The contradiction between these two sets of results indicates that autophagy became defective, that is, that a reduction in the induction, maturation and degradation of autophagy was

induced. Therefore, we assessed the degradative activity in tBHP-treated H9c2 cells with a set of fluorescent dyes—MDC, AO, and lysotracker red. These fluorescent dyes can label acid vacuoles that utilize acid hydrolases to degrade the materials enclosed within them. Concentration- and time-dependent decreases in the fluorescent intensities of these dyes were observed (Fig. 4). Inversely related to the decreases in these acid vacuole markers, the fluorescent intensity of mitotracker green increased (Fig. 4a3,b3) (This dye is an indicator of mitochondrial mass regardless of membrane potential). Furthermore, the reduction of autophagic degradation capacity would provide a reasonable explanation for the accumulation of LC3-II (Fig. 3b). Finally, the decrease in DJ-1 content induced by oxidative stress in H9c2 cells may play a vital role in the regulation of mitochondrial mass via defects in autophagy.

In conclusion, our observations indicate that oxidative stress induced accumulation of mitochondria in H9c2 cells. Changes in mtDNA copy number showed that mitochondrial biogenesis may not directly determine the increase in mitochondrial mass. Rather, aberrant autophagy has been observed in the present work. These defects in the induction, maturation, and degradation of autophagy can induce mitochondrial accumulation as measured by fluorescent labels.

ACKNOWLEDGMENTS

This study was partially supported by the National Natural Science Foundation of China, Key Program 30930105 and General Program 31070740; New Century Excellent Talents in University to JGL; and the 985 and 211 Projects of Xi'an Jiaotong University.

REFERENCES

Agnello M, Morici G, Rinaldi AM. 2008. A method for measuring mitochondrial mass and activity. Cytotechnology 56:145–149.

Anderson S, Bankier AT, Barrell BG, de Bruijn MH, Coulson AR, Drouin J, Eperon IC, Nierlich DP, Roe BA, Sanger F, Schreier PH, Smith AJ, Staden R, Young IG. 1981. Sequence and organization of the human mitochondrial genome. Nature 290:457–465.

Andersson BS, Vidal RF, Sundberg M, Rajs J, Sotonyi P. 1996. Hydroperoxide-induced nucleotide degradation and adenosine formation in isolated rat cardiomyocytes. Toxicology 106:39–48.

Apostolova N, Gomez-Sucerquia LJ, Moran A, Alvarez A, Blas-Garcia A, Esplugues JV. 2010. Enhanced oxidative stress and increased mitochondrial mass during efavirenz-induced apoptosis in human hepatic cells. Br J Pharmacol 160:2069–2084.

Ballinger SW. 2005. Mitochondrial dysfunction in cardiovascular disease. Free Radic Biol Med 38:1278–1295.

Beal MF, Lin MT. 2006. Mitochondrial dysfunction and oxidative stress in neurodegenerative diseases. Nature 443:787–795.

Biederbick A, Kern HF, Elsasser HP. 1995. Monodansylcadaverine (MDC) is a specific in vivo marker for autophagic vacuoles. Eur J Cell Biol 66:3–14.

Chazotte B. 2011. Labeling lysosomes in live cells with LysoTracker. Cold Spring Harb Protoc pdb prot5571. 2011(2):210–212.

Chen H, Chan DC. 2009. Mitochondrial dynamics—Fusion, fission, movement, and mitophagy—In neurodegenerative diseases. Hum Mol Genet 18:R169–R176.

Codogno P, Meijer AJ. 2005. Autophagy and signaling: Their role in cell survival and cell death. Cell Death Differ 12:1509–1518.

Cookson MR, Mccoy MK. 2011. DJ-1 regulation of mitochondrial function and autophagy through oxidative stress. Autophagy 7:531–532.

Cuervo AM, Wong E. 2010. Autophagy gone awry in neurodegenerative diseases. Nat Neurosci 13:805–811.

Dai DF, Johnson SC, Villarin JJ, Chin MT, Nieves-Cintron M, Chen T, Marcinek DJ, Dorn GW II, Kang YJ, Prolla TA, Santana LF, Rabinovitch PS. 2011. Mitochondrial oxidative stress mediates angiotensin II-induced cardiac hypertrophy and Galphaq overexpression-induced heart failure. Circ Res 108:837–846.

Drahota Z, Krivakova P, Cervinkova Z, Kmonickova E, Lotkova H, Kucera O, Houstek J. 2005. *Tert*-butyl hydroperoxide selectively inhibits mitochondrial respiratory-chain enzymes in isolated rat hepatocytes. Physiol Res 54:67–72.

Giasson BI, Hao LY, Bonini NM. 2010. DJ-1 is critical for mitochondrial function and rescues PINK1 loss of function. Proc Natl Acad Sci USA 107:9747–9752.

Goldman SJ, Taylor R, Zhang Y, Jin S. 2010. Autophagy and the degradation of mitochondria. Mitochondrion 10:309–315.

Gorbunov NV, Tyurina YY, Salama G, Day BW, Claycamp HG, Argyros G, Elsayed NM, Kagan VE. 1998. Nitric oxide protects cardiomyocytes against *tert*-butyl hydroperoxide-induced formation of alkoxyl and peroxyl radicals and peroxidation of phosphatidylserine. Biochem Biophys Res Commun 244:647–651.

Guarino RD, Dike LE, Haq TA, Rowley JA, Pitner JB, Timmins MR. 2004. Method for determining oxygen consumption rates of static cultures from microplate measurements of pericellular dissolved oxygen concentration. Biotechnol Bioeng 86:775–787.

Haidara K, Morel I, Abalea V, Gascon Barre M, Denizeau F. 2002. Mechanism of tert-butylhydroperoxide induced apoptosis in rat hepatocytes: Involvement of mitochondria and endoplasmic reticulum. Biochim Biophys Acta 1542:173–185.

Hausenloy DJ, Ong SB. 2010. Mitochondrial morphology and cardiovascular disease. Cardiovasc Res 88:16–29.

Hayashi T, Ishimori C, Takahashi-Niki K, Taira T, Kim YC, Maita H, Maita C, Ariga H, Iguchi-Ariga SM. 2009. DJ-1 binds to mitochondrial complex I and maintains its activity. Biochem Biophys Res Commun 390:667–672.

He C, Klionsky DJ. 2009. Regulation mechanisms and signaling pathways of autophagy. Annu Rev Genet 43:67–93.

Khan HA. 2003. Bioluminometric assay of ATP in mouse brain: Determinant factors for enhanced test sensitivity. J Biosci 28:379–382.

Kimes BW, Brandt BL. 1976. Properties of a clonal muscle cell line from rat heart. Exp Cell Res 98:367–381.

Krebiehl G, Ruckerbauer S, Burbulla LF, Kieper N, Maurer B, Waak J, Wolburg H, Gizatullina Z, Gellerich FN, Woitalla D, Riess O, Kahle PJ, Proikas-Cezanne T, Kruger R. 2010. Reduced basal autophagy and impaired mitochondrial dynamics due to loss of Parkinson's disease-associated protein DJ-1. PLoS ONE 5:e9367.

Krivakova P, Labajova A, Cervinkova Z, Drahota Z. 2007. Inhibitory effect of *t*-butyl hydroperoxide on mitochondrial oxidative phosphorylation in isolated rat hepatocytes. Physiol Res 56:137–140.

Lavandero S, Parra V, Verdejo H, del Campo A, Pennanen C, Kuzmicic J, Iglewski M, Hill JA, Rothermel BA. 2011. The complex interplay between mitochondrial dynamics and cardiac metabolism. J Bioenerg Biomembr 43:47–51.

Lee HC, Wei YH. 2005. Mitochondrial biogenesis and mitochondrial DNA maintenance of mammalian cells under oxidative stress. Int J Biochem Cell Biol 37:822–834.

Lee HC, Yin PH, Lu CY, Chi CW, Wei YH. 2000. Increase of mitochondria and mitochondrial DNA in response to oxidative stress in human cells. Biochem J 348(Pt 2):425–432.

Lee HC, Yin PH, Chi CW, Wei YH. 2002. Increase in mitochondrial mass in human fibroblasts under oxidative stress and during replicative cell senescence. J Biomed Sci 9:517–526.

Lee CF, Liu CY, Hsieh RH, Wei YH. 2005. Oxidative stress-induced depolymerization of microtubules and alteration of mitochondrial mass in human cells. Ann N Y Acad Sci 1042:246–254.

Lee CF, Chen YC, Liu CY, Wei YH. 2006. Involvement of protein kinase C delta in the alteration of mitochondrial mass in human cells under oxidative stress. Free Radic Biol Med 40:2136–2146.

Lemasters JJ. 2005. Perspective—Selective mitochondrial autophagy, or mitophagy, as a targeted defense against oxidative stress, mitochondrial dysfunction, and aging. Rejuvenation Res 8:3–5.

Long LH, Hoi A, Halliwell B. 2010. Instability of, and generation of hydrogen peroxide by, phenolic compounds in cell culture media. Arch Biochem Biophys 501:162–169.

Michel S, Wanet A, De Pauw A, Rommelaere G, Arnould T, Renard P. 2011. Crosstalk between mitochondrial (dys)function and mitochondrial abundance. J Cell Physiol 227:2297–2310.

Mizushima N. 2007. Autophagy: Process and function. Genes Dev 21:2861–2873.

Nojiri H, Shimizu T, Funakoshi M, Yamaguchi O, Zhou H, Kawakami S, Ohta Y, Sami M, Tachibana T, Ishikawa H, Kurosawa H, Kahn RC, Otsu K, Shirasawa T. 2006. Oxidative stress causes heart failure with impaired mitochondrial respiration. J Biol Chem 281:33789–33801.

Otsu K, Nakai A, Yamaguchi O, Takeda T, Higuchi Y, Hikoso S, Taniike M, Omiya S, Mizote I, Matsumura Y, Asahi M, Nishida K, Hori M, Mizushima N. 2007. The role of autophagy in cardiomyocytes in the basal state and in response to hemodynamic stress. Nat Med 13:619–624.

Rothermel BA, Iglewski M, Hill JA, Lavandero S. 2010. Mitochondrial fission and autophagy in the normal and diseased heart. Curr Hypertens Rep 12:418–425.

Salvioli S, Ardizzoni A, Franceschi C, Cossarizza A. 1997. JC-1, but not DiOC6(3) or rhodamine 123, is a reliable fluorescent probe to assess delta psi changes in intact cells: Implications for studies on mitochondrial functionality during apoptosis. FEBS Lett 411:77–82.

Sardao VA, Oliveira PJ, Holy J, Oliveira CR, Wallace KB. 2007. Vital imaging of H9c2 myoblasts exposed to tert-butylhydroperoxide—Characterization of morphological features of cell death. BMC Cell Biol 8:11.

Shen W, Liu K, Tian C, Yang L, Li X, Ren J, Packer L, Cotman CW, Liu J. 2008. R-alpha-lipoic acid and acetyl-L-carnitine complementarily promote mitochondrial biogenesis in murine 3T3-L1 adipocytes. Diabetologia 51:165–174.

Shokolenko I, Venediktova N, Bochkareva A, Wilson GL, Alexeyev MF. 2009. Oxidative stress induces degradation of mitochondrial DNA. Nucleic Acids Res 37:2539–2548.

Stankiewicz M, Jonas W, Hadas E, Cabaj W, Douch PG. 1996. Supravital staining of eosinophils. Int J Parasitol 26:445–446.

Stroikin Y, Dalen H, Loof S, Terman A. 2004. Inhibition of autophagy with 3-methyladenine results in impaired turnover of lysosomes and accumulation of lipofuscin-like material. Eur J Cell Biol 83:583–590.

Thomas KJ, McCoy MK, Blackinton J, Beilina A, van der Brug M, Sandebring A, Miller D, Maric D, Cedazo-Minguez A, Cookson MR. 2011. DJ-1 acts in parallel to the PINK1/parkin pathway to control mitochondrial function and autophagy. Hum Mol Genet 20:40–50.

Tolkovsky AM. 2009. Mitophagy. Biochim Biophys Acta 1793:1508–1515.

Uchida T, Nishimura M, Saeki T, Watanabe Y. 1994. Effects of membrane lipid peroxidation by tert butyl hydroperoxide on the sodium current in isolated feline ventricular myocytes. Heart Vessels 9:227–234.

Uchiyama Y, Shibata M, Koike M, Yoshimura K, Sasaki M. 2008. Autophagy-physiology and pathophysiology. Histochem Cell Biol 129: 407–420.

Victor VM, Apostolova N, Herance R, Hernandez-Mijares A, Rocha M. 2009. Oxidative stress and mitochondrial dysfunction in atherosclerosis: Mitochondria-targeted antioxidants as potential therapy. Curr Med Chem 16:4654–4667.

Watkins SJ, Borthwick GM, Arthur HM. 2011. The H9C2 cell line and primary neonatal cardiomyocyte cells show similar hypertrophic responses in vitro. In Vitro Cell Dev Biol Anim 47:125–131.

Yoon Y, Galloway CA, Jhun BS, Yu TZ. 2011. Mitochondrial dynamics in diabetes. Antioxid Redox Signal 14:439–457.

Zhang L, Shimoji M, Thomas B, Moore DJ, Yu SW, Marupudi NI, Torp R, Torgner IA, Ottersen OP, Dawson TM, Dawson VL. 2005. Mitochondrial localization of the Parkinson's disease related protein DJ-1: Implications for pathogenesis. Hum Mol Genet 14:2063–2073.

Zorzano A, Liesa M, Palacin M. 2009a. Mitochondrial dynamics in mammalian health and disease. Physiol Rev 89:799–845.

Zorzano A, Liesa M, Palacin M. 2009b. Role of mitochondrial dynamics proteins in the pathophysiology of obesity and type 2 diabetes. Int J Biochem Cell Biol 41:1846–1854.